Research Article

Radiation Tolerant 3D Laser Scanner for Structural Inspections in Nuclear Reactor Vessels and Fuel Storage Pools

Luigi De Dominicis [ID],[1] **Mario Carta,**[2] **Massimiliano Ciaffi,**[1] **Luca Falconi,**[2] **Mario Ferri de Collibus,**[1] **Massimo Francucci,**[1] **Massimiliano Guarneri** [ID],[1] **Marcello Nuvoli,**[1] **and Fabio Pollastrone** [ID][1]

[1]*Department of Fusion and Technology for Nuclear Safety and Security, ENEA Centro Ricerche Frascati, Via E. Fermi 45, Frascati 00044, Italy*
[2]*Department of Fusion and Technology for Nuclear Safety and Security, ENEA Centro Ricerche Casaccia, Via Anguillarese 301, Rome 00123, Italy*

Correspondence should be addressed to Luigi De Dominicis; luigi.dedominicis@enea.it

Accurate and timely assessment of displacements and/or structural damages in nuclear reactor vessels' components is a key action in routine inspections for planning maintenance and repairs but also in emergency situations for mitigating consequences of nuclear incidents. Nevertheless, all these components are maintained underwater and reside in high-radiation fields thus imposing harsh operative conditions to inspection devices which must cope with effects such as Cerenkov radiation background, Total Ionizing Radiation (TID), and occlusions in the detectors' field of view. To date, ultrasonic techniques and video cameras are in use for inspection of components' integrity and with measurements of volumetric and surface crack opening displacements, respectively. The present work reports the realization of a radiation tolerant laser scanner and the results of tests in a nuclear research reactor vessel for acquisition of 3D models of critical components. The device, qualified for underwater operation and for withstanding up to 1 MGy of TID, is based on a 515 nm laser diode and a fast-scanning electro-optic unit. To evaluate performances in a significant but controlled environment, the device has been deployed in the vessel of a research reactor operated by ENEA in the Casaccia Research Centre in Rome (Italy). A 3D model of the fuel rods assembly through a cooling water column of 7 m has been acquired. The system includes proprietary postprocessing software that automatically recognizes components of interest and provides dimensional analysis. Possible application fields of the system stretch to dimensional analysis also in spent nuclear fuel storage pools.

1. Introduction

Safety of the nuclear reactor vessels (RVs) is one of the major concerns of nuclear power plants operators. RV is a steel cylinder containing the reactor core with the fuel rods assembly, systems controlling the reaction, and tubes and nozzles for fluids' circulations. All these components are maintained underwater and reside in high radiation fields. Although the material used for these components has been selected to resist to corrosion and structural faults, they need periodical inspections for checking the status and to plan maintenance or repair interventions. Nonroutine inspections are required when the system reports criticalities, when external events (i.e., earthquakes) may be supposed to induce structural damages, or in the extreme case of loss of the reactor control. Nevertheless, RV inspection is one of the most challenging tasks in nuclear installations. In fact, the activity is performed underwater and, for in-service and out of control conditions, in a highly radiation contaminated environment. In-service inspections are the preferred solutions for operators to avoid the financial losses of reactor shutdown, while are a constrained choice when the reactor is out of control. Ultrasonic testing has been extensively used in nuclear industry for volumetric

examinations of components [1, 2]. Nevertheless, case studies demonstrate that many detected defects in nuclear reactor components are from crack initiating in the surface of the elements and with successive propagation in the interior of the structure [3]. This has led to ascertain the capacity of video cameras to detect small cracks before they grow to a size that may impair the correct functionality of the component. Radiation-hardened submersible video cameras are now available for the nuclear industry and qualified up to 2 MGy of TID [4] at a dose rate of 1 kGy/h for ^{60}Co irradiation conditions. They usually have a Light Emitting Diode (LED) ring around the lens to provide illumination and are operated remotely. Studies and tests demonstrate that their performances in detecting cracks are strongly influenced by lighting conditions that are hardly reproducible, also for the Cerenkov radiation background contribution, thus making it difficult to compare acquisitions taken at different times to evaluate how the Crack Opening Displacement (COD) evolves. In addition [3], their performances in terms of dimensional analysis accuracy rapidly deteriorate for operative distances larger than 3 m. Within this framework and building upon the consolidated evidence that for terrestrial applications 3D laser scanners perform better than video cameras in terms of operative range and accuracy, ENEA has developed an Amplitude-Modulated (AM) 3D laser scanning imaging system for nuclear applications, being the device qualified for underwater operations and to withstand up to 1 MGy of TID as certified by tests conducted by manufacturers on critical device components. The ENEA device marks a step forward in the development of laser-based imaging systems for nuclear applications where systems so far available are not radiation resistance rated and based on the triangulation technique that is intrinsically limited to short range imaging [5].

The device is intended for improved inspection capabilities in nuclear reactor vessels by enabling extended operative range, no lighting conditions dependence of data, high accuracy in COD detection, and 3D acquired model's comparison with CAD drawings. Possible application fields of the device extend to inspection in spent nuclear fuel storage pools and eventually also installed on autonomous underwater vehicles. The device gathers together the proven track record of ENEA in developing 3D laser scanner imaging systems for terrestrial and subsea environments and for applications under vacuum conditions in fusion chambers [6]. The advantages of the amplitude modulation technique for underwater operation of 3D laser imaging have been previously demonstrated both theoretically and experimentally [7–9].

In order to reduce the effect of background Cerenkov radiation, the system is based on a 515 nm laser source. The apparatus has been tested in operative conditions inside the vessel of the research nuclear reactor TRIGA (Training Research Isotopes General Atomics) RC1 (Reactor Casaccia 1) at the ENEA research centre of Casaccia (Rome). TRIGA RC1 is a 1 MWth reactor with a cylindrical structure moderated and cooled by water. The apparatus encompasses an optical head to be immersed in the vessel and an electronic unit for control that is operated remotely.

The present work describes the system realization and the results of the experimental campaign at TRIGA RC1.

2. Materials and Methods

2.1. Amplitude Modulated 3D Laser Imaging in Underwater. In an AM laser 3D imaging system, the intensity of a spatially collimated laser beam is sinusoidally modulated at a frequency *f*. The range *d* of the target point illuminated by the laser is determined by measuring the phase shift Ω (phase channel) of the reflected radiation by the target's surface and with respect to a reference signal. The range *d* is retrieved from the measurable quantity Ω with the formula

$$d = \frac{\Omega c}{(4\pi n f)},\tag{1}$$

where *c* is the vacuum speed of light and *n* is the medium index of refraction. Range is inversely proportional to ω, thus making range error Δd inversely proportional to square of *f*. Consequently, higher modulation frequencies improve system performances. Nevertheless, an issue related to the AM laser 3D imaging system is range aliasing, which means a range ambiguity originating from the periodic nature of the modulation and that does not allow to discriminate between two range measurements differing for multiples of 2π in Ω. Aliasing is usually resolved by adopting a double modulation frequency technique, where a Low Frequency (LF) and a High Frequency (HF) of modulation are used in the system [10]. The low frequency allows for disambiguation of the range, while the high frequency provides an accurate measurement once disambiguation has been resolved.

A 3D image of the target surface can be recorded by sweeping the laser onto the target's whole surface, collecting the cloud of range information *d* and reconstructing the 3D model with a proper software. The 3D rendering is intrinsically dimensional, meaning that it is possible to measure dimensions and distances of target surface features directly on the 3D model. The device allows also for the recording of the 2D image of the target surface and in a scale of grey proportional to surface reflectivity at the wavelength of the laser (intensity channel). Another key property of the method is that it does not require an external illumination due to the fact that the laser beam is the probe and its reflected portion the signal to be detected. The main advantage with respect to video cameras is the possibility to accurately compare 3D models acquired at different times and to quantitatively evaluate differences. When operating underwater, like in the case of RV inspections, it must be carefully considered the detrimental effect on range evaluation of the optical noise originating from the portion of the laser beam backscattered by the water. The effect is more and more pronounced as water turbidity increases due to the presence of dissolved matter. If *k* is the water attenuation coefficient and *n* is the water index of refraction, it is possible to demonstrate [8] that backscattered laser intensity I_b behaves like a Butterworth's (equation (2)) low pass filter with a modulation cut-off frequency $f_c = kc/2\pi n$:

$$I_b \propto \frac{1}{\sqrt{1 + f/f_c}}, \tag{2}$$

This implies that, for modulation frequencies $f > f_c$, the contribution from water backscattering is minimized with enhancement in terms of the operative range of the system and 3D model accuracy. Theoretical calculations, as reported in Figure 1, show that, for a typical value of $k = 0.5\,m^{-1}$, as in reactor vessels, $f_c = 17.9\,MHz$, a modulation frequency well within the range of commercial laser sources where amplitude modulation frequencies up to 200 MHz may be attained.

These theoretical considerations underpin the development of an AM 3D laser imaging system for applications in RVs where components have to be inspected from meters of distance due to physical constraints, which prevent installations of imaging systems in proximity of the reactor core. From the operational point of view, water in RVs is almost maintained at high purity and, hence, with low values of k because this is the most important factor in preventing degradation of aluminium clad fuel elements and of other structural components in water-cooled research reactors [11]. Most relevant is the uncertainty related to the water index of refraction n, that is, a function of the operating temperature T. The $n(T)$ dependence has been studied by several authors [12, 13], and the results demonstrate that, for pure water, it decreases about 1.5% in the 0°C–100°C range and with a typical value of 1.33 at 25°C. It follows that, for precise measurements in RVs, it is recommended to estimate water temperature and calculate the value of $n(T)$ to be used in equation (1) accordingly.

2.2. The AM 3D Laser Imaging Device for Nuclear Applications. The radiation tolerant AM 3D laser imaging system developed at ENEA and tested in the TRIGA RC1 nuclear research reactor consists of two separated modules, an active and a passive one (probe), as shown in the scheme in Figure 2.

The passive module is the part of the system qualified to operate underwater and in radiation environments. It consists basically of a watertight housing of stainless steel with aluminium gaskets and equipped with one optical window. Inside are allocated lenses, mirrors, and optical fibres for laser beam steering and deflection to accomplish the scanning of the inspected areas. All the optical components are treated with a hard-rad dielectric coating (SiO_2-Ta_2O_5) tested up to 5 MGy. The motors for tilt (TR-14 Pytron) and pan (TR-20 Pytron) of the scanning mirror are radiation hardened with radiation-resistant lubricant (Ultratherm 2000) and tested up to 1 MGy. The electric microswitches, used as end of run and reference, are made of polyether ether ketone (PEEK), golden bronze, and ruby. A watertight stainless-steel tube connects the active to the passive module, leading the optical fibres and electrical cables inside. All the copper wires are insulated with Kapton and are 10 m long, and the optical fibres in the system are radiation hardened and with a Radiation Induced Attenuation, at 515 nm and for a TID of 1 MGy, in the range
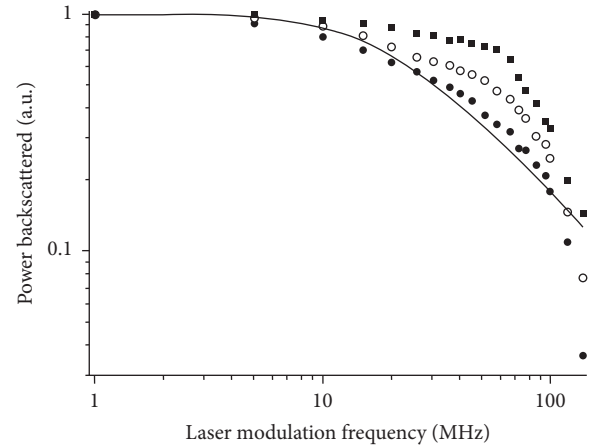

Figure 1: Normalized backscattered power vs. laser modulation frequency measured for different water attenuation coefficients: (●) $k = 0.5\,m^{-1}$, (○) $k = 1.1\,m^{-1}$, and (■) $k = 2.1\,m^{-1}$. The continuous curve is the plot of Butterworth's filter function in equation (2) for $k = 0.5\,m^{-1}$.

1–1.5 dB/m. For the laser beam, transmission single mode fibres are mounted, while for signal reception, a multimode bundle (7 fibres, 400 μm diameter each) are used to increase the depth of field and reduce the bending radius.

The active module includes the laser, a compact diode laser at 515 nm of wavelength with maximum CW power of 20 MW (Omicron LuxX® Laser Series) and possibility of analogic amplitude modulation up to 200 MHz. In order to eliminate the aliasing effect, the laser was simultaneously amplitude modulated at a low frequency LF = 10 MHz and at a high frequency HF = 200 MHz.

The module also hosts an Avalanche Photodiode Detector (APD) for signal detection, the front-end electronic, a 600 MHz lock-in amplifier, and the scanning motors' controller. An interference filter is positioned in front of the APD for eliminating the Cerenkov radiation background.

The performances of the device in terms of range error Δd as a function of the distance of the target have been simulated with an in-house developed calculation code, and the results are shown in Figure 3 with noncontaminated and contaminated water (TID = 1 MGy) and for $n = 1.33$, $k = 0.05\,m^{-1}$, laser power of 7 MW, and integration time of the lock-in amplifier that equals to 10 ms.

Range error increases with target distance and more rapidly for the case in which the system is subject to a TID of 1 MGy. For the simulation under irradiation conditions and for a target distance less than 5 m, the range error is still below to 1 mm.

3. Results and Discussion

The TRGA RC1 is a research reactor with an active core currently loaded with 111 U-ZrH fuel rods (8.5 weight %U and 20% enrichment), moderated and cooled with demineralized water, and equipped with B_4C control rods. The RV is cylindrical with a height of 8 m and diameter 2.5 m and accessible from the above (see Figure 4). A major concern in planning the experimental campaign was the
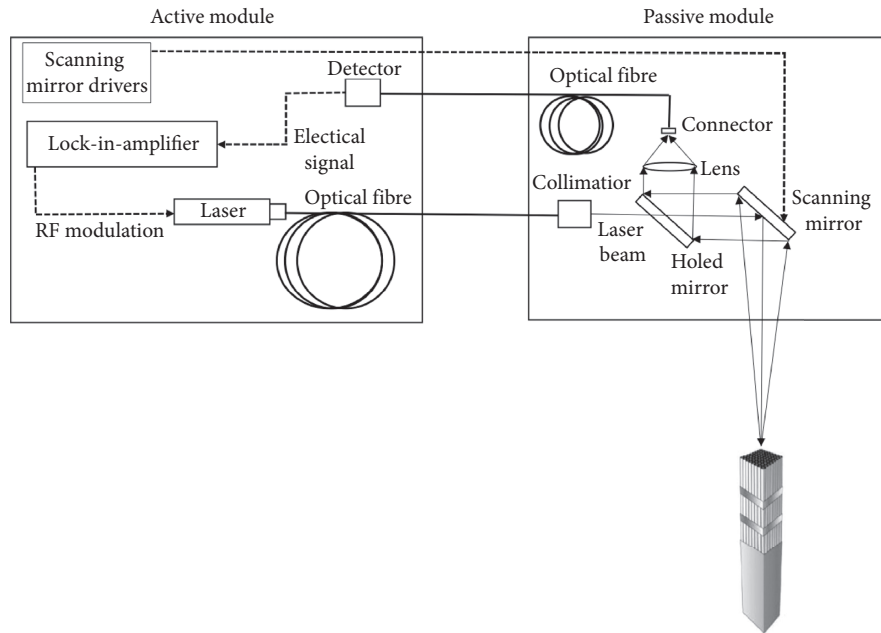
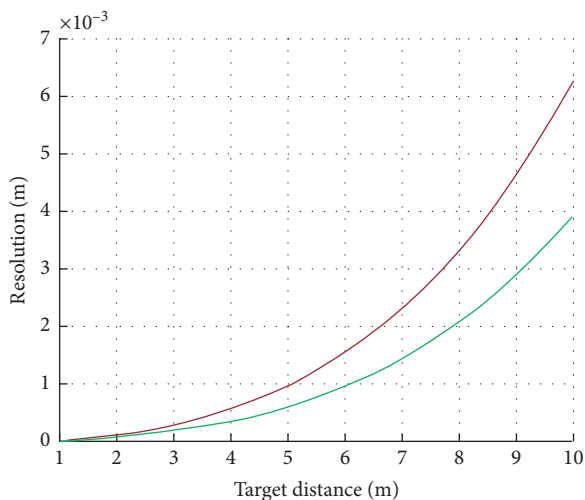Figure 2: Scheme of the ENEA radiation tolerant AM 3D laser imaging system.

Figure 3: Device performance simulation for water with $k = 0.05 \, \mathrm{m}^{-1}$: the green curve represents noncontaminated water and red curve represents contaminated water, and TID = 1 MGy.
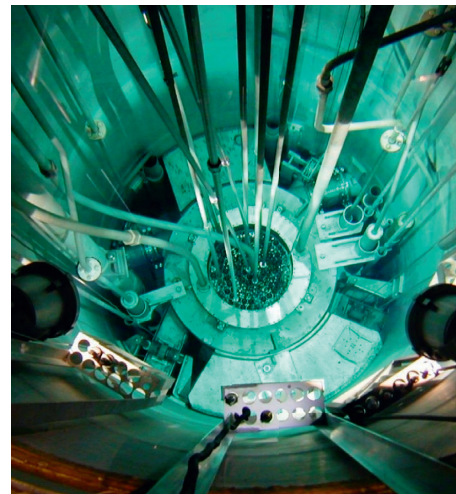

Figure 4: Picture of the TRIGA RC1 reactor vessel with the fuel rods' circular array on the bottom and taken with a high-quality commercial photographic camera.

activation by thermal neutrons in TRIGA RC1 of the aluminium in the watertight housing of the passive module. In fact, neutrons capture of ^{27}Al forms ^{28}Al that decays with beta emission to ^{28}Si * which subsequently de-excites, via gamma emission at 1.779 MeV, to ^{28}Si. The reaction has a large thermal neutron capture cross-section of around 12 barns. In light of this, it was decided to carry on the measurements with the reactor shutdown and in a pure gamma radiation field. At the beginning of the experimental campaign, the gamma dose rate measured at the top of the reactor vessel was 0.17 Gy/h, and this value has been monitored all along the permanence of the 3D laser systems in the cooling water. On this basis, it has been estimated that the TID absorbed by the device is 14 Gy.

A picture of the passive module immersed in the TRIGA RC1 RV during the experimental campaign and of the active module is shown in Figure 5 left and right, respectively.

The passive module was installed just below the water surface of the TRIGA RC1 RV and operated remotely with a proprietary software installed on a PC in the reactor control room.

The 2D intensity and 3D model images acquired during the experimental campaign are shown in Figures 6 and 7, respectively.

In the 2D image produced by the intensity channel of the device, it has an enhanced contrast with respect to the one in Figure 4 acquired with a high-quality photographic camera. This is due to the concurrent elimination of the effect of the

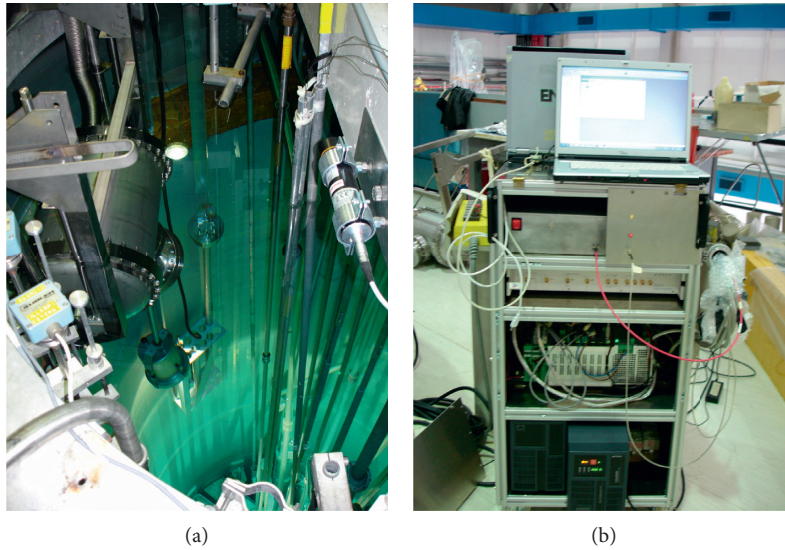(a)   (b)

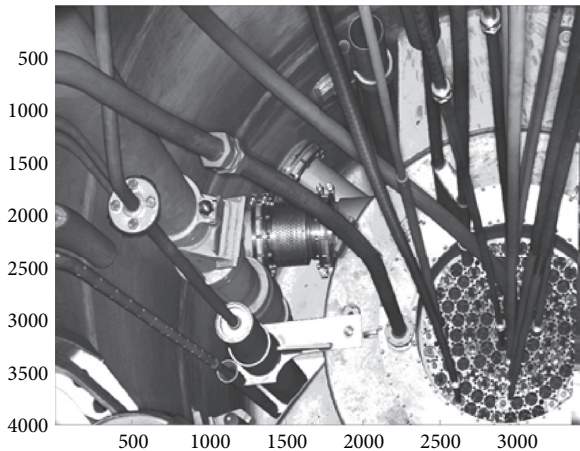FIGURE 5: (a) Passive module immersed in the TRIGA RC1 RV. (b) The active module during system installation at TRIGA RC1.

FIGURE 6: The 2D image of the TRIGA RC1 reactor vessel as acquired with the intensity channel of the device.

FIGURE 7: The 3D model of the TRIGA RC1 reactor vessel as acquired with the phase channel of the device.

Cerenkov background radiation and of the diffused illuminating lamps' light from the backscattered modulated laser light. The 2D image has a 16 megapixels resolution obtained by working with a collimated laser beam at the limit of diffraction and with the mirrors' scanning motors operating at the finest resolution step (acquisition time 65 s.). The 2D image presents some inhomogeneities in the grey scale along some curved and long length elements due to the non-Lambertian behaviour of metal surfaces' reflectance. In fact, higher reflectance is measured for nearly normal incidence with respect to the plane surface and indicating a reflectance specular component dominating over the Lambertian one.

The nuclear scanner is also equipped by a postprocessing data analysis tool, which can elaborate a complete 3D model of the scanned scene with a 216 bits grey levels' intensity information. Another feature of the data analysis software, helpful to detect possible cracks or deteriorations of the parts composing the structure, is the possibility to automatically
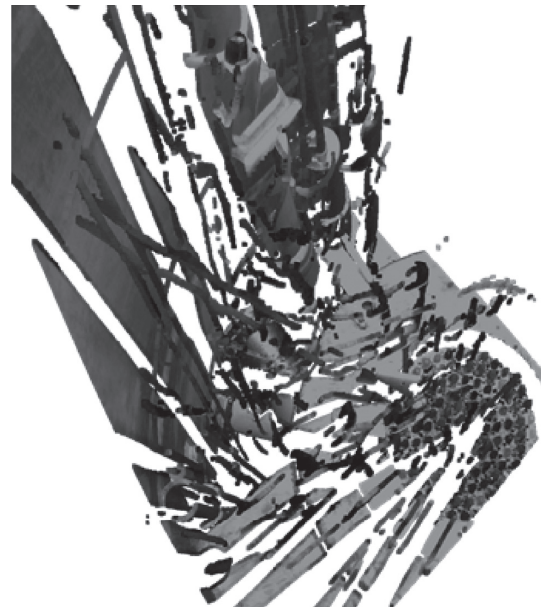
recognize interested components and make measures of their dimensions. Figure 8 shows the intensity image used for the automatic shapes' detection [14]; and with the green circles indicating the selected features for measuring the diameter of the fuel rods allocations in the reactor core assembly. The average estimation of the circle's diameter is 43 mm with an error (represented by the standard deviation of the measures) of ± 1.5 mm with respect to dimensions by the initial design. The algorithm for the dimensional analysis exploits the range information as stored in the phase measurement channel (see equation (1)). In the calculation code, it has been assumed a conventional value of 1.33 for n.

As visible in the figure, not all the detected shapes fit perfectly the interested elements: this is caused mainly by the

(a)   (b)
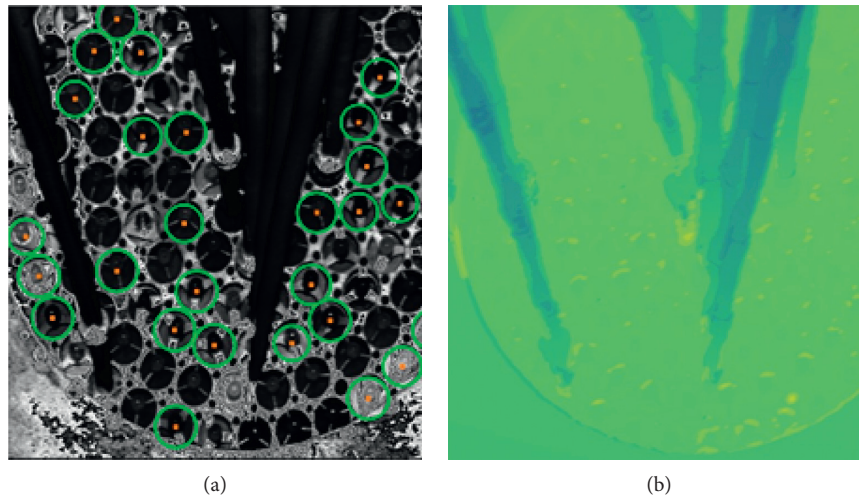
FIGURE 8: (a) Intensity image with detected shapes overlapped; (b) Depth map for estimating the dimensions of the detected shapes.

complexity of the structure, represented by the presence of occlusions of several pipes crossing the angle of view of the scanner and by the reflections of the metallic surfaces composing some elements placed perpendicularly to the scanning optical system.

Critically, the proprietary calculation code has the potentiality to compare quantitatively 3D models taken at different times and even at different device operating positioning, in order to elaborate differences at the millimetric level to identify the insurgence of cracks or to evaluate their evolution over time.

4. Conclusions

Building upon the experience in developing AM 3D laser imaging systems for underwater applications, ENEA has realized a device qualified for operation in radiation-contaminated water and up to a TID = 1 MGy. The capacity of the device to operate in a nuclear reactor vessel has been demonstrated in a research facility and in a pure gamma radiation field for avoiding issues related to aluminium components' activation by fission neutrons. The results of this experimental campaign at the TRIGA RC1 nuclear reactor of ENEA demonstrate the capacity of the system to accomplish dimensional analysis at 7 m of distance of the target and with a millimetric resolution. This result is in line with the system performances simulated with a proprietary calculation code, thus demonstrating that we reached the experimental limits with the current technological components available. It is worth mentioning that despite the ENEA device is qualified for a TID threshold nearly half that of the most advanced radiation-hardened video camera; the presented results demonstrating that it operates satisfactorily at larger distances from the target guarantee an extended operative lifetime when inspecting the fuel rods assembly and due to the fact that the radiation dose decreases sharply with the distance from the reactor core. The present results pave the way for further scientific and technological investigations to further improve the device for dimensional

structural analysis in nuclear power plants' reactor vessels and spent fuel storage pools.

Data Availability

The data used to support the findings of this study are included within the article.

Conflicts of Interest

The authors declare that there are no conflicts of interest regarding the publication of this paper.

Acknowledgments

References

[1] E. J. Sullivan, M. T. Anderson, and W. Norris, "In-service inspection ultrasonic testing of reactor pressure vessel welds for assessing flaw density and size distribution per 10 CFR 50.61a, alternate fracture toughness requirements for protection against pressurized thermal shock," in *Proceedings of the ASME 2011 Pressure Vessels and Piping Conference*, pp. 125–130, Tokyo, Japan, July 2011.

[2] H. J. Meyer and W. Rath, "Ultrasonic equipment for inspection of reactor pressure vessels in service," *Non-Destructive Testing*, vol. 7, no. 1, pp. 19–24, 1974.

[3] S. E. Cumblidge, M. T. Anderson, S. R. Doctor, F. A. Simonen, and A. J. Elliott, "As of remote visual methods to detect cracking in reactor components," *U.S. NuclearRegulatory Commission NUREG/CR-6943*, vol. 23, 2007.

[4] https://www.mirion.com/products/r942-camera-system.

[5] https://newtonlabs.com/nuke_nm300uw_landpg.htm.

[6] F. Crescenzi, F. Pollastrone, G. Mugnaini, C. Neri, and P. Rossi, "IVVS probe mechanical concept design," *Fusion Engineering and Design*, vol. 98, pp. 1597–1600, 2015.

[7] L. De, "3D vision, ranging and range gating"," in *Subsea Opticsand Imaging*, J. Watson and O. Zielinski, Eds., WoodHead publishing, Cambridge, UK, 2013.

[8] L. De Dominicis, M. Ferri de Collibus, G. Fornetti et al., "Improving underwater imaging in an Amplitude modulated laser system with radio frequency control technique"" *Journal ofthe European Optical Society - Rapid Publications*, vol. 5, pp. 100041–100045, 2010.

[9] L. Bartolini, L. De Dominicis, M. Ferri de Collibus et al., "Underwater three-dimensional imaging with an amplitude-modulated laser radar at a 405nm wavelength"" *Applied Optics*, vol. 44, no. 33, pp. 7130–7135, 2005.

[10] C. Zhang, S. Liu, Z. Zhang et al., "Comprehensive ranging disambiguation for amplitude-modulated continuous-wave laser scanner," in *Proceedings of the SPIE 11352, Optics and Photonics for Advanced Dimensional Metrology*, Bordeaux, France, April 2020.

[11] IAEA Nuclear Energy Series No. NP-T-52, *Good Practice for Water Quality Management in research Reactors and Spent Fuel Storage Facilities*, IAEA Nuclear Energy Series No. NP-T-52, Vienna, Austria, 2011.

[12] G. Abbate, U. Bernini, E. Ragozzino, and F. Somma, "The temperature dependence of the index of Refraction of water," *Journal of Physics D*, vol. 11, 1978.

[13] A. N. Bashkatov and E. A. Genina, "Water refractive index in dependence on temperature and wavelength: a Simple approximation, saratov fall meeting 2002: optical technologies in biophysics and medicine iv," *The Society of Photo-optical Instrumentation Engineers*, vol. 50, 2003.

[14] H. K. Yuen, J. Princen, J. Dlingworth, and J. Kittler, "A comparative study of hough transform methods for circle finding," *Journal on Advancement of Technology*, vol. 29, no. 6, pp. 1–29, 2013.